Pergamon

*Int. J. Solids Structures* Vol. 34, No. 22, pp. 2887–2904, 1997

0020–7683/97 $17.00 + .00

PII: S0020–7683(96)00202–8

# STRESS CONCENTRATIONS AND MICROFRACTURING PATTERNS IN A BRITTLE-ELASTIC SOLID WITH INTERACTING PORES OF DIVERSE SHAPES

I. TSUKROV and M. KACHANOV
Department of Mechanical Engineering, Tufts University, Medford, MA, 02155 U.S.A.

(*Received* 25 *October* 1995; *in revised form* 14 *August* 1996)

**Abstract**—Elastic interactions between holes of diverse eccentricities, as well as between holes and cracks, are analyzed. We examine physical effects produced by interactions and the impact of hole eccentricities on these effects. Mixtures of strongly interacting holes of diverse eccentricities and sizes are of particular interest. Patterns of stress concentrations in such mixtures imply certain microfracturing patterns in materials with multiple defects. © 1997 Elsevier Science Ltd.

## 1. INTRODUCTION

It is well known that holes act as stress concentrators. Stress concentrations at a *single* hole have been extensively studied for various hole shapes (Kolosov, 1909 and Inglis, 1913 for a 2-D elliptical hole; Muskhelishvili, 1953 and Savin, 1961 for various non-elliptical shapes; Edwards, 1951 for the general 3-D spheroids).

For *interacting* holes, the following works should be mentioned. Numerical solutions for several symmetric arrangements have been produced (see, for example, Ling, 1947; Haddon, 1967; Horii and Nemat-Nasser, 1985; Duan *et al.*, 1986). Computer simulations for arrays of arbitrarily located holes and cracks have been recently produced by Hu *et al.* (1993); the same issues were addressed by Fond *et al.* (1995) who also examined the impact of boundaries in a finite plate and the effects of crack closure. Interacting holes in the limit of small spacings were considered by Duan *et al.* (1986) and by Zimmerman (1988); both works suggested similar asymptotic formulas but with different numerical factors. Hwu and Liao (1994) applied the boundary element method to the analysis of interacting holes and inclusions; the emphasis of their analysis was on the computational aspects and on the accuracy of the procedure rather than on the physical effects produced by interactions.

In all the mentioned works, except for the work of Hwu and Liao (1994), the interacting holes were assumed to be *circular*. In real materials, though, pores often have strongly non-circular shapes. Moreover, *mixtures* of holes of diverse shapes are typical (for example, pores and microcracks). We examine the impact of these factors on a simple model of elliptical holes. This shape includes circles and cracks as limiting cases. Some preliminary results of the present work were reported by Tsukrov and Kachanov (1994).

The present work focuses on the following issues:

—impact of holes' eccentricities on the interaction effects;
—"large hole–small hole" interactions;
—likely microfracturing patterns in *mixtures* of defects of diverse shapes.

To study interactions, we employ the Neumann-Schwarz alternating method, or stress "feedbacks" (see, for example, Sokolnikoff, 1956) that has previously been applied to interacting *cracks* (Rajiyah and Atluri, 1989 and other works). It appears to be more efficient and accurate (particularly, for closely spaced strongly interacting holes) than series expansions of tractions on holes with coefficients of expansion found from a large system of equations, or the finite element method. The implementation of the alternating method

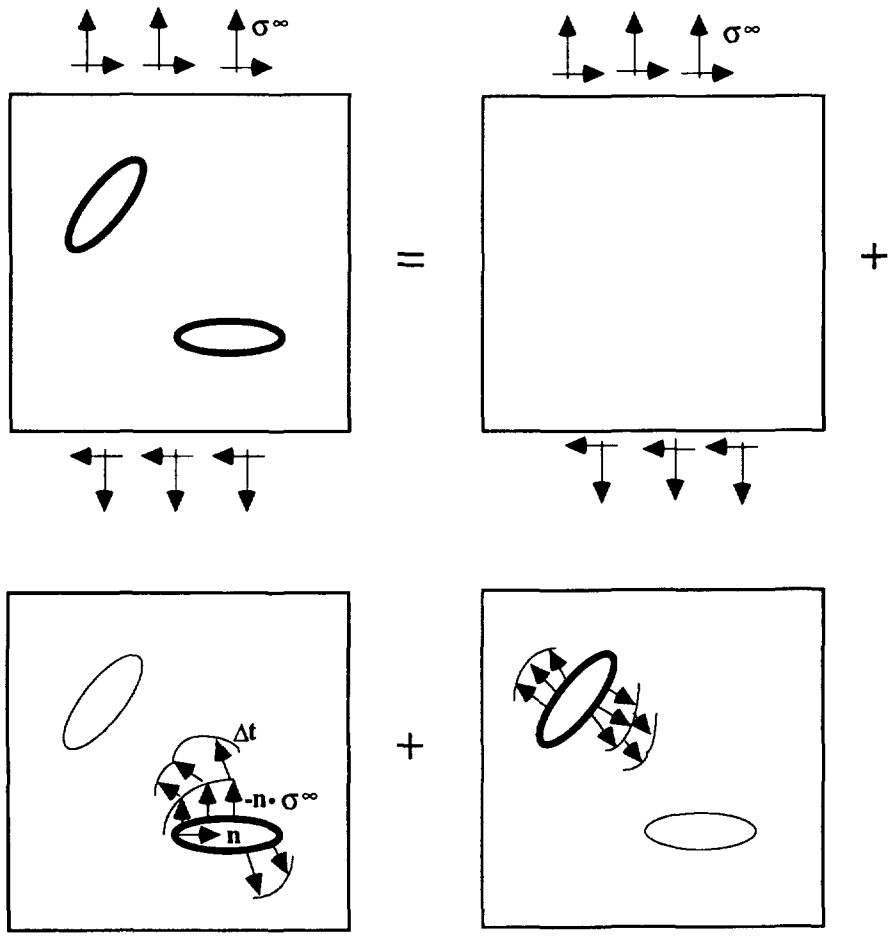


Fig. 1. Stress superposition for interacting holes.

requires fundamental solutions, i.e., the full stress fields produced by a point force on a boundary of a single hole in an infinite solid.

The analysis is limited to the 2-D configurations. Besides providing a simple model of much more complex 3-D problems, this analysis is relevant for porous space of "tubular" structure that occurs, for example, in some geomaterials (Zimmerman, 1991).

## 2. COMPUTATIONAL PROCEDURE, FUNDAMENTAL SOLUTIONS AND TEST PROBLEMS

Using stress superpositions, we represent the problem of $N$ holes in an infinite plate with stresses $\sigma_{ij}^{\infty}$ at infinity as a superposition of the uniform stress state $\sigma_{ij}^{\infty}$ and $N$ subproblems with one hole each. In the $k$-th subproblem, the $k$-th hole is loaded by the $\sigma_{ij}^{\infty}$-induced traction $\mathbf{t}^{(k)} = -\mathbf{n}^{(k)} \cdot \boldsymbol{\sigma}^{\infty}$ (where $\mathbf{n}^{(k)}$ is the unit normal to the $k$-th hole boundary $l^{(k)}$ directed inside the hole) plus the interaction tractions

$$\sum_i \Delta \mathbf{t}^{(ik)}$$

induced at the site of $l^{(k)}$ in a continuous material by all the other, $i$-th, holes, in the $i$-th subproblems (Fig. 1).

The interaction tractions $\Delta \mathbf{t}^{(ik)}$ can be found by the alternating technique. They are taken to be zeros in the 0-th iteration (non-interacting holes) and are re-calculated, using the results of previous iteration, at each step. At $j$-th step, the correction to $\Delta \mathbf{t}^{(ik)}$ represents the influence on the $k$-th hole of the tractions on $l^{(i)}$ calculated at $(j-1)$-th step; it is found

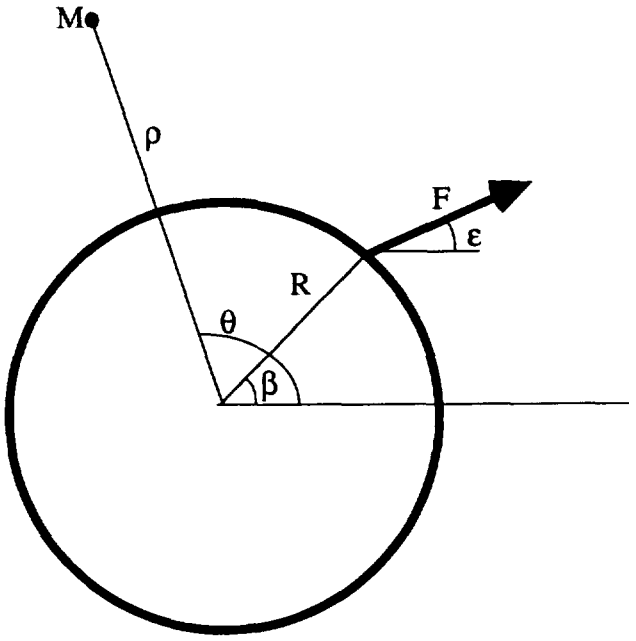


Fig. 2. Point force at the boundary of a circular hole.

by integration of the influence of the point force applied at a point of $l^{(i)}$ over the contour of $l^{(i)}$. Thus, the procedure requires knowledge of the full stress field generated by a point force of an arbitrary direction applied at a boundary of an isolated hole in an infinite plate (fundamental solution).

To find the fundamental solution for an elliptical hole with semiaxes $a$ and $b$, we use the transformation

$$z = R(\zeta + m/\zeta) \tag{1}$$

which maps conformally the exterior of the ellipse in the complex $z$-plane onto the exterior of a unit circle in the $\zeta$-plane [it is denoted: $R=(a+b)/2$, $m=(a-b)/a+b)$]. The stresses can be obtained by the modification of Kolosov-Muskhelishvili's technique, in which stresses are expressed in terms of only one stress function $\varphi(\zeta)$ (see Green and Zerna, 1954):

$$\left.\begin{aligned} \sigma_{\xi\xi}+\sigma_{\eta\eta} &= 4\left\{\frac{\varphi'(\zeta)}{z'(\zeta)}+\overline{\frac{\varphi'(\zeta)}{z'(\zeta)}}\right\} \\ \sigma_{\xi\xi}-\sigma_{\eta\eta}+2i\sigma_{\xi\eta} &= -4\frac{\bar{\zeta}}{\zeta z'(\zeta)}\frac{\mathrm{d}}{\mathrm{d}\bar{\zeta}}\left\{[z(\zeta)-z(1/\bar{\zeta})]\overline{\frac{\varphi'(\zeta)}{z'(\zeta)}}-\varphi(1/\bar{\zeta})\right\} \end{aligned}\right\}. \tag{2}$$

The stress function $\varphi(\zeta)$ for the point force $F_1+iF_2$ applied at the point of the boundary of the elliptical hole that corresponds to the point $e^{i\beta}$ of the unit circle in the $\zeta$-plane can be derived by the standard complex variable technique (Muskhelishvili, 1953) as follows:

$$\varphi(\zeta) = \frac{F_1+iF_2}{4\pi}\left[\frac{\kappa}{\kappa+1}\log\zeta-\log(\beta-\zeta)\right] \tag{3}$$

where $\kappa=(3-\nu)/(1+\nu)$ for plane stress and $\kappa=3-4\nu$ for plane strain.

In the simplest case of the *circular* hole of radius $R$ loaded by a point force at the boundary (Fig. 2), the stress field simplifies to the expressions

Table 1. Hoop stress for two interacting circular holes at the points of closest ($\sigma_{near}$) and farthest ($\sigma_{far}$) separation, as a function of spacing between the holes. Comparison of our results with results of other authors

| $d/R$ | $\sigma_{near}$ | $\sigma_{far}$ | Ling, 1947 | Haddon, 1967 | Horii, Nemat-Nasser, 1985 | Duan *et al.*, 1986 | Zimmerman, 1988 |
|---|---|---|---|---|---|---|---|
| 0.01 | 28.87 | 3.734 | | | | | 27.4 |
| 0.02 | 20.32 | 3.684 | | | | 20.35 | 19.4 |
| 0.1 | 8.688 | 3.511 | | 8.689 | | 8.69 | 8.68 |
| 0.2 | 6.106 | 3.407 | | 6.106 | | 6.11 | |
| 0.4 | 4.422 | 3.295 | | 4.423 | 4.423 | 4.42 | |
| 1.0 | 3.264 | 3.150 | 3.264 | 3.264 | 3.264 | 3.281 | |
| 2.0 | 3.020 | 3.066 | 3.066 | 3.066 | | 3.079 | |

$$\sigma_{\rho\rho} = \frac{F}{2\pi\rho}(1-r^2)\left\{2\frac{\kappa}{\kappa+1}\cos(\varepsilon-\theta)+\frac{1}{T}[r\cos(\varepsilon-\beta)-2\cos(\varepsilon-\theta)]\right.$$
$$\left.+\frac{1}{T^2}[-\cos(\varepsilon-\theta)+2r\cos(\varepsilon-\beta)-r^2\cos(\varepsilon+\theta-2\beta)]\right\};$$
$$\sigma_{\rho\theta} = \frac{F}{2\pi\rho}(1-r^2)\left\{-2\frac{\kappa}{\kappa+1}\sin(\varepsilon-\theta)-\frac{1}{T}r\sin(\varepsilon-\beta)\right.$$
$$\left.+\frac{1}{T^2}[\sin(\varepsilon-\theta)-2r\sin(\varepsilon-\beta)+r^2\sin(\varepsilon+\theta-2\beta)]\right\};$$
$$\sigma_{\theta\theta} = \frac{F}{2\pi\rho}\left\{2\frac{\kappa}{\kappa+1}(1-r^2)\cos(\varepsilon-\theta)+\frac{1}{T}[r(3+r^2)\cos(\varepsilon-\beta)-2(1+r^2)\cos(\varepsilon-\theta)]\right.$$
$$\left.+\frac{1-r^2}{T^2}[\cos(\varepsilon-\theta)-2r\cos(\varepsilon-\beta)+r^2\cos(\varepsilon+\theta-2\beta)]\right\} \tag{4}$$

where $T = 1-2r\cos(\beta-\theta)+r^2$ and $r = R/\rho$. (Note that Dundurs and Hetenyi, 1961 and Hetenyi and Dundurs, 1962 gave solutions for the point forces normal and tangential to the hole in a less convenient form.)

We first apply the alternating technique to the test configuration of two circular holes of equal sizes under remote tension in the direction normal to the line connecting the hole centers. Results for this configuration have been obtained earlier by other numerical methods; we use them to check the accuracy and the rate of convergence of our procedure. Note that most of the available results are for the distances $d$ between the holes that are not too small, so that the interaction effect (the difference between the values given in Table 1 and the stress amplification factor of 3 for a single isolated hole) remains relatively weak. As seen from Table 1, our procedure remains efficient at quite small distances (of the order of 1/100 of the hole radius $R$) when the interaction effect is very strong (stress amplification factor of about 30).

In the limit of *spacing between holes* $\to 0$, this configuration was considered by Zimmerman (1988) who arrived at the asymptotic expression $\sigma_{hoop}/\sigma_\infty = 1.94/\sqrt{d/(2R)}$. Duan *et al.* (1986) gave a numerical study of closely spaced holes. Note that both mentioned works are limited to the case of circular holes of equal size. Our results are in full agreement with those of Duan *et al.* and are slightly (about 5%) higher than the ones of Zimmerman.

We note a peculiar, counterintuitive effect produced by the interaction of two circular holes: at certain spacings between the holes, $\sigma_{far} > \sigma_{near}$. This happens when the spacing between holes is sufficiently large and the interaction effect is weak (the last line of Table 1), so that it may not have significant physical consequences. Nevertheless, we find this observation interesting. The effect seems to be rooted in the structure of the stress field associated with a single circular hole: as seen from Fig. 3, the stress $\sigma_{xy}$ induced by hole 1

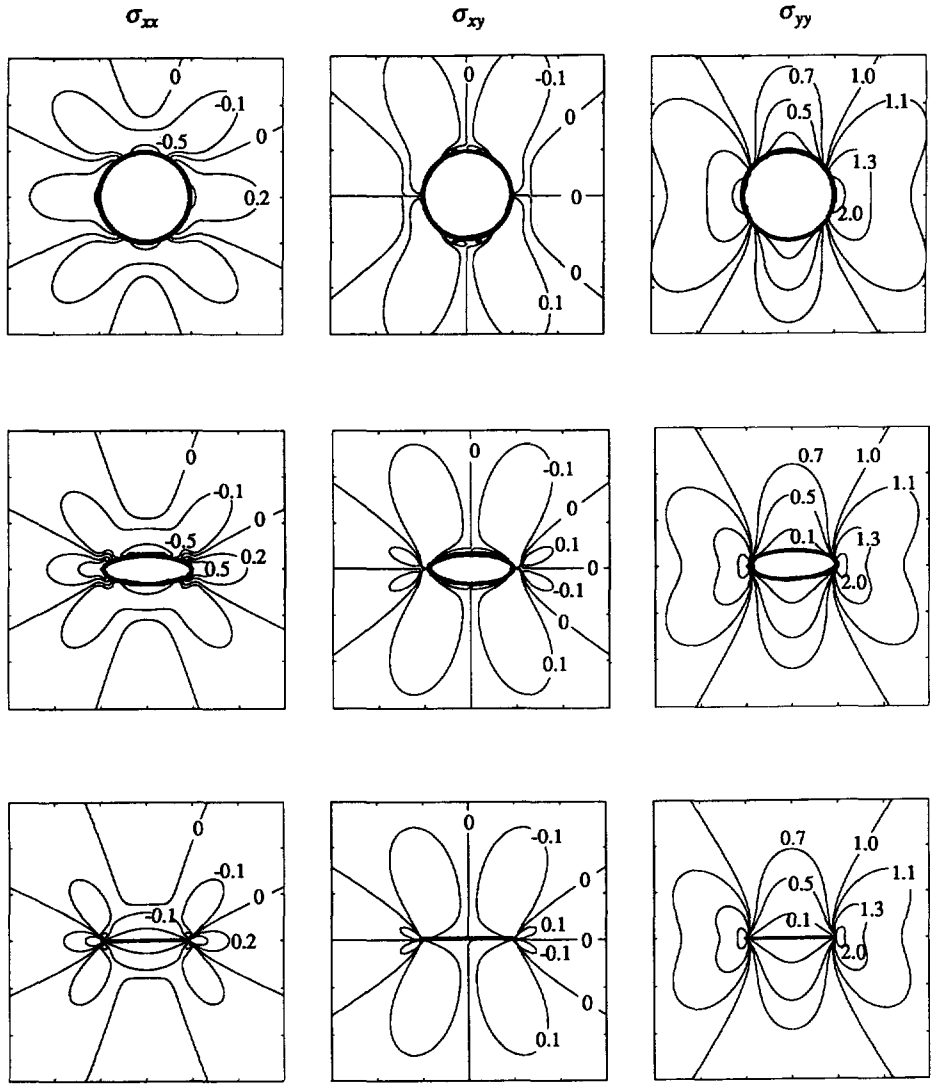


Fig. 3. "Standard" stress fields around an elliptical hole under remote tension $\sigma_{yy}$ of unit intensity for three hole eccentricities, $b/a = 1, 1/3$ and 0 (lines of equal stress levels).

at the site of hole 2 may be higher at the *outer* (farthest) edge of hole 2 than at the inner one, giving rise to the higher $\sigma_{yy}$ at this edge.

## 3. STRESS FIELDS ASSOCIATED WITH ONE ELLIPTICAL HOLE

The stress fields associated with a single isolated hole placed in the otherwise homogeneous stress field are of fundamental importance for the interaction problems—their structure determines most of the interaction effects. These fields, corresponding to placing the hole into the stress fields of uniform tension and uniform shear, will be called "standard" fields in the text to follow. They are shown in Figs 3 and 4.

Indeed, in the first (and dominant, in most cases) stress "feedback" of the alternating method, the impact of hole 1 on hole 2 is found by placing hole 2 into the "standard" field of hole 1. (For example, the zone of reduced/elevated $\sigma_{yy}$ around hole 1 under a uniaxial tension $\sigma_{yy}^{\infty}$ is the zone of shielding/amplification, in the sense that hole 2 placed into this zone is subjected to a reduced/elevated tension and thus experiences a shielding/amplifying influence of hole 1.) This is the reason why the "standard" fields are shown in detail here (Figs 3, 4)—examination of their structure is often sufficient to qualitatively estimate the interaction effects. We note that different loading conditions produce different zones of shielding/amplification, so that the same arrangement of holes may produce shielding under

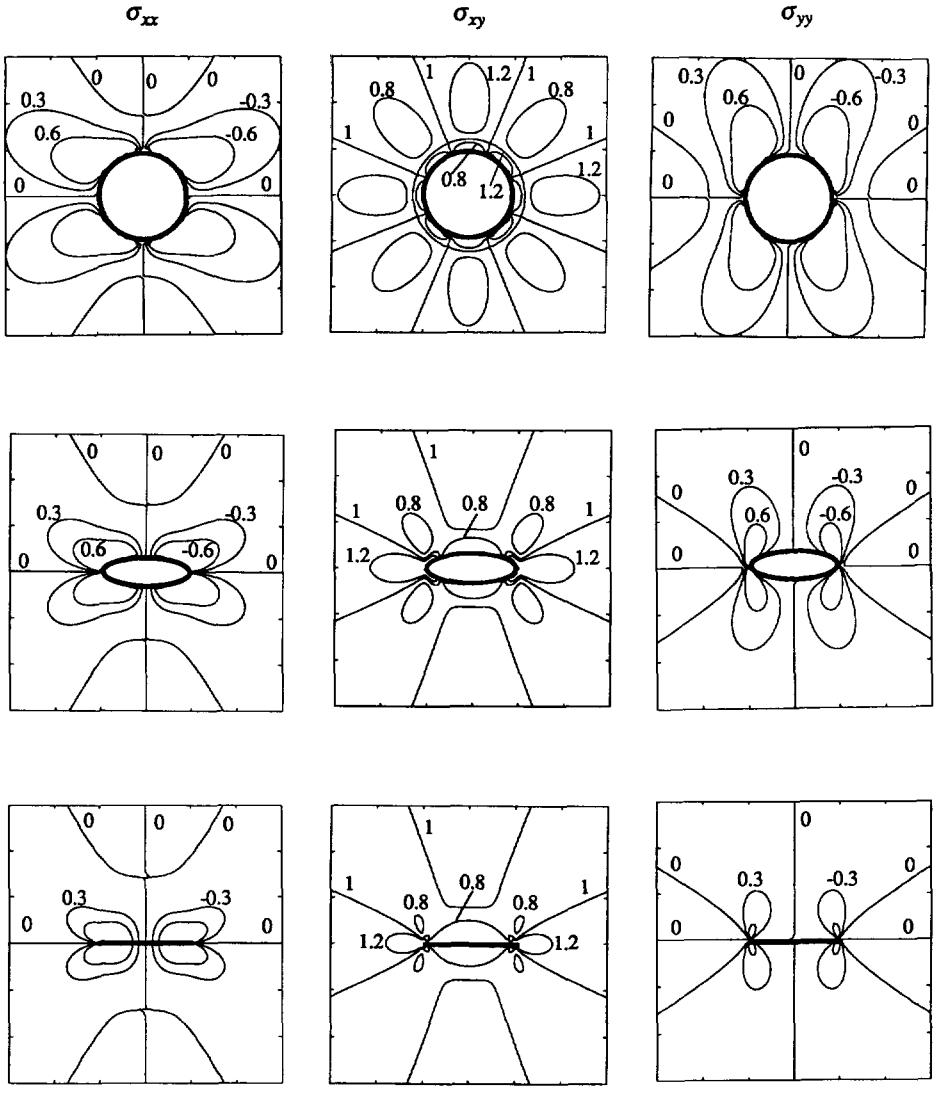


Fig. 4. "Standard" stress fields around an elliptical hole under remote shear $\sigma_{xy}$ of unit intensity for three hole eccentricities, $b/a = 1$, 1/3 and 0 (lines of equal stress levels).

remote tension and amplification under remote shear. These effects are discussed in the next section.

The solution for an elliptical hole in an infinite elastic plate under uniform tension was given by Kolosov (1909) for the special case of remote tension in the direction normal to one of the ellipse's axes and by Inglis (1913) in the case of remote tension in an arbitrary direction; see Muskhelishvili (1919, 1953) for details and Maugis (1992) for graphical illustrations. Here, we explicitly show the structure of the stress fields, since it directly relates to the mechanics of interactions.

Figure 3 shows the "standard" stress fields associated with one elliptical hole under remote tension normal to one of axes of the hole. An important observation is that, for elongated holes, the zones of amplification (elevated $\sigma_{yy}$) under remote tension are compact and intense, whereas the zones of shielding (reduced $\sigma_{yy}$) are larger and less intense. The underlying reason is best illustrated by the limiting case of cracks, where it is most strongly pronounced. Introduction of a crack into a field of uniform tension does not change the average over the body stress (follows from the divergence theorem). Hence, contributions into this average from the zones of amplified $\sigma_{yy}$ that contain crack tip singularities should be balanced by contributions of the opposite sign from the zones of shielding where $\sigma_{yy}$ is finite. Therefore, zones of shielding should be larger than the ones of amplification. Similar observations hold for mode II loading: relatively small zones of intense amplification of

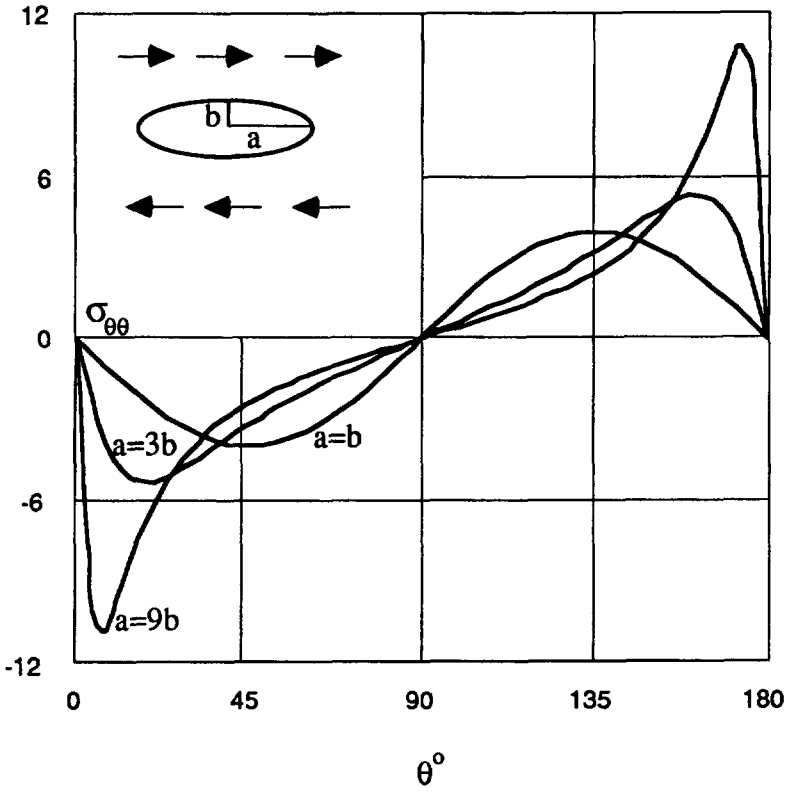


Fig. 5. Hoop stress at the boundary of an elliptical hole under remote shear. Note that the location of the point of maximal concentration is asymmetric and depends on the eccentricity.

$\sigma_{xy}$ are balanced by larger zones of mild shielding (not exceeding 20% at any point), see Fig. 4. As far as $\sigma_{xx}$ and $\sigma_{xy}$ fields under remote tension (or $\sigma_{xx}$, $\sigma_{yy}$ fields under remote shear) are concerned, the sizes of the zones of negative and positive stresses are comparable.

Another interesting observation concerning elliptical holes is that, under remote shear, the location of the point of maximal hoop stress on the hole boundary depends on ellipse's eccentricity (Fig. 5).

## 4. IMPACT OF HOLE ECCENTRICITIES ON SHIELDING AND AMPLIFYING INTERACTIONS

Interactions between holes may produce both stress shielding and stress amplification, depending on (1) mutual positions of holes, (2) hole eccentricities and (3) mode of remote loading. As discussed in Section 3, these effects are rooted in the structure of the "standard" fields. They are illustrated here by several representative configurations. Note that for cracks, such effects were discussed in detail by Kachanov (1993).

(*a*) *Two identical collinear holes under remote tension* (*Figs 6, 7*). The interaction effect is the one of stress amplification (similarly to the case of collinear cracks). It rapidly decreases as the spacing between holes increases. This short range character of the collinear interactions can be immediately related to the structure of the "standard" stress fields: as seen from Fig. 3, the stress $\sigma_{yy}$ rapidly decreases along the $x$-axis. Another interesting observation is that, if the holes are transformed from cracks to circles (while keeping the spacing between the holes fixed), the interaction effect, characterized by the ratio of the hoop stress at the hole tips to its value for an isolated hole, becomes stronger (although the absolute value of the hoop stress decreases).

(*b*) *Two identical stacked holes under remote tension* (*Fig. 8*). Similarly to the case of cracks, the interaction effect is the one of stress shielding. In contrast with the collinear interactions, the strength of interaction decreases rather slowly, as the spacing between the holes increases. This long range character of stacked interactions is, again, directly seen

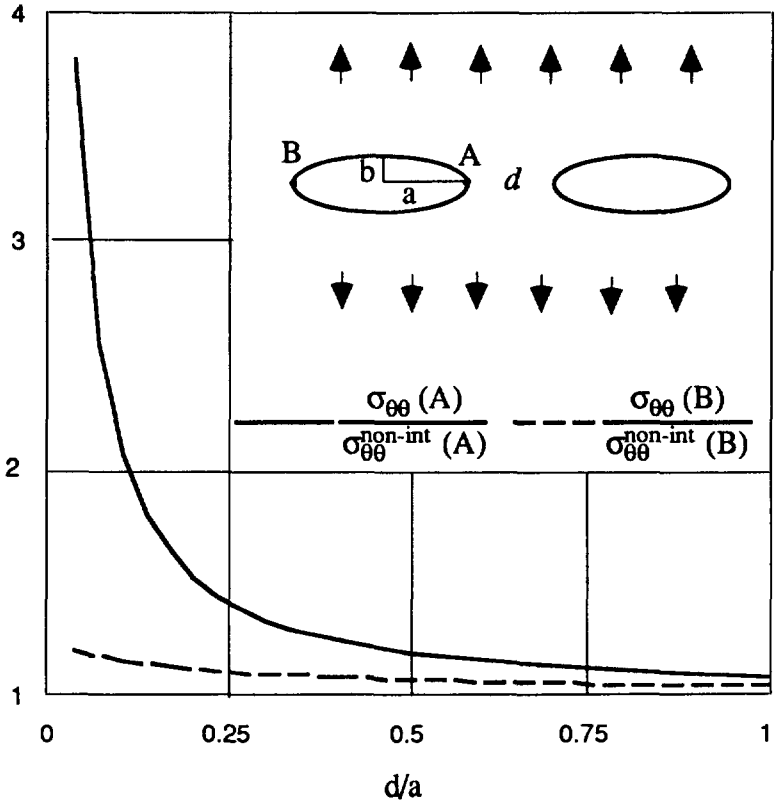


Fig. 6. Two identical collinear holes (eccentricity $b/a = 1/3$) under remote tension. Stress concentration (normalized to the one for a single hole) as a function of spacing between the holes.

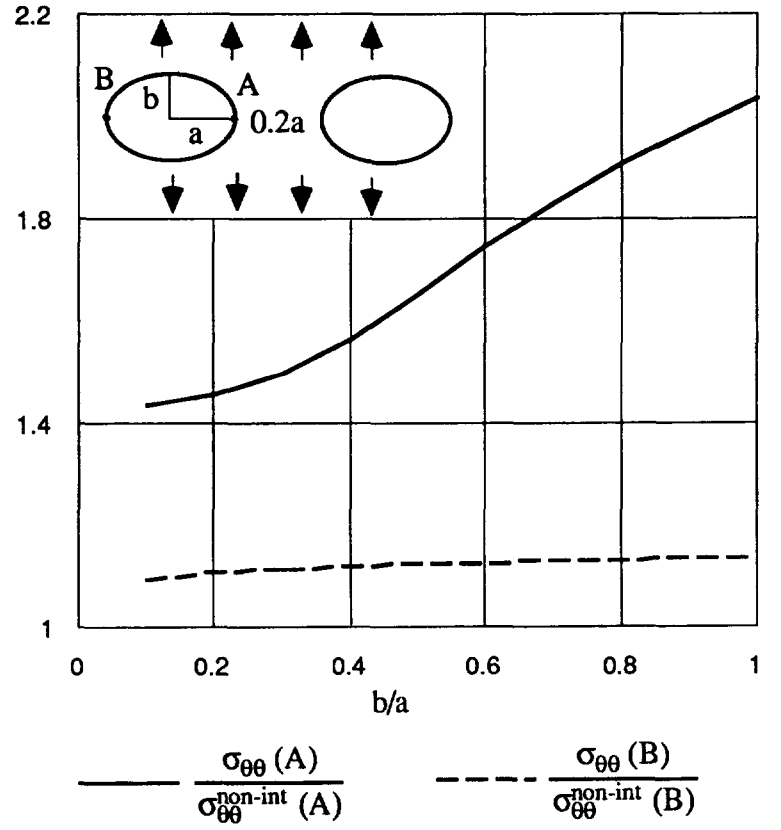


Fig. 7. Two identical collinear holes under remote tension. Stress concentration (normalized to the one for a single hole) as a function of holes' eccentricity.

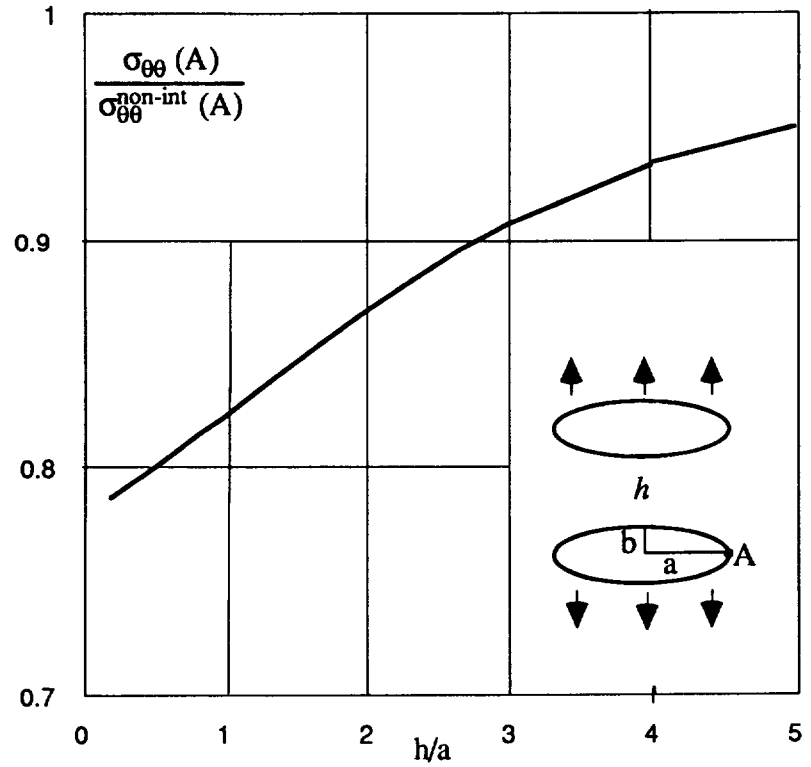


Fig. 8. Two identical stacked holes (eccentricity $b/a = 1/3$) under remote tension. Stress concentration (normalized to the one for a single hole) as a function of spacing between the holes.

from the structure of the "standard" fields: the stress $\sigma_{yy}$ decreases in the $y$-direction substantially slower than in the $x$ direction.

(*c*) *Interaction under shear loading: collinear configuration.* In the collinear configuration (Fig. 9), the interaction effect is the one of amplification (similarly to the case of remote tension). In addition to the increase of the maximal hoop stress, the interaction moves the point of the hole boundary where it occurs (point $A$ in Fig. 9).

(*d*) *Interaction under shear loading: stacked configuration.* In contrast with the case of remote tension, the interaction effect is the one of amplification (Fig. 10). This illustrates the dependence of the interaction effect on the mode of loading.

## 5. INTERACTION OF A LARGE HOLE WITH A SMALL HOLE. LIKELY MICROFRACTURING PATTERNS

In the problem of large hole–small hole interaction, the point of the highest tensile hoop stress (and, therefore, the point of likely fracture initiation) may occur either at the smaller hole or at the larger one. This depends on the shapes of the holes and is best illustrated by two limiting cases—circles and cracks. In these two cases, the results are opposite. Indeed, for a single circular hole, the maximum hoop stress under remote tension $p$ is $3p$: the concentration factor of 3 is independent of the hole size. Consider now the system "large circular hole–small circular hole" (Fig. 11a). Since the impact of the larger hole on the smaller one is stronger than vice versa, the highest hoop stress hoop stress occurs at the boundary of the smaller hole. Calculations show that the differences in $\sigma_{\theta\theta}$ at two holes may be quite substantial: for the ratio of 3 of the holes' radii, $\sigma_{max}$-values at the larger and smaller holes, respectively, are: (3.001, 3.279), (3.203, 4.851) and (3.468, 6.262) at the distances between holes of 1, 1/3 and 1/5 of the larger hole radius. Therefore, as the critical load is reached, it is the smaller hole that will fracture (and propagate towards the larger one).

In the system "large crack–small crack", collinear arrangement (Fig. 11b), the opposite is true: $K_I(B) > K_I(A)$ (Yokobori *et al.*, 1965). Thus, at the critical load, fracture starts at

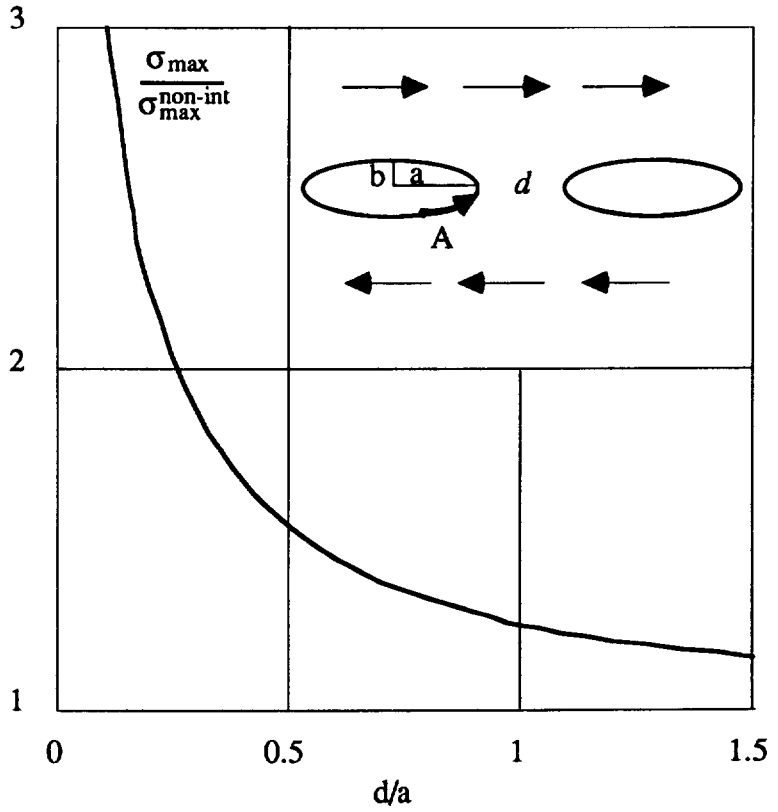


Fig. 9. Interaction of two identical collinear holes (eccentricity $b/a = 1/3$) under remote shear. Stress concentration (normalized to the one for a single hole) as a function of spacing between the holes. The interaction moves the point $A$ of the maximal hoop stress in the direction shown.

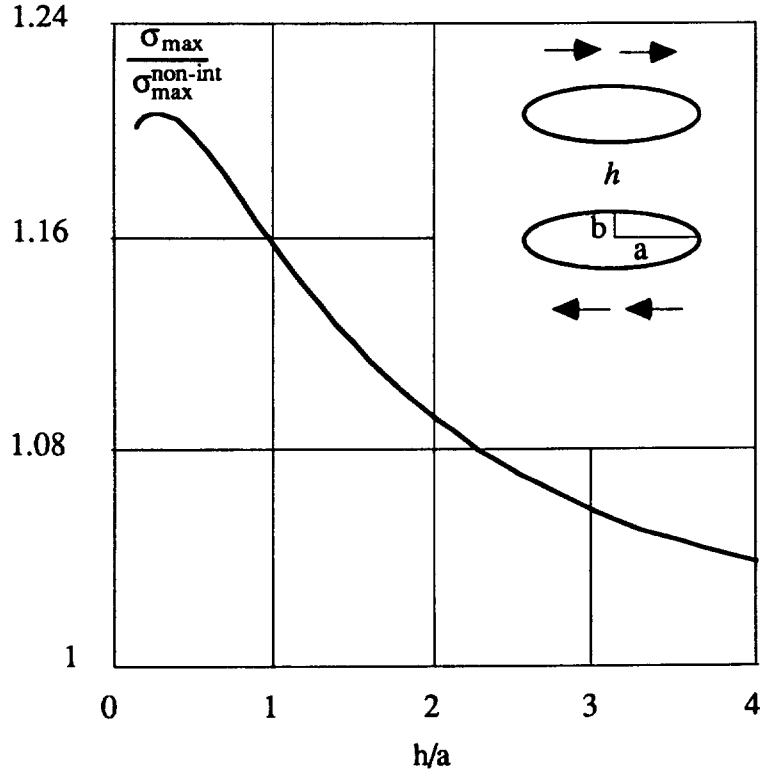


Fig. 10. Stress amplification for two identical stacked holes (eccentricity $b/a = 1/3$) under remote shear. Stress concentration (normalized to the one for a single hole) as a function of spacing between the holes.

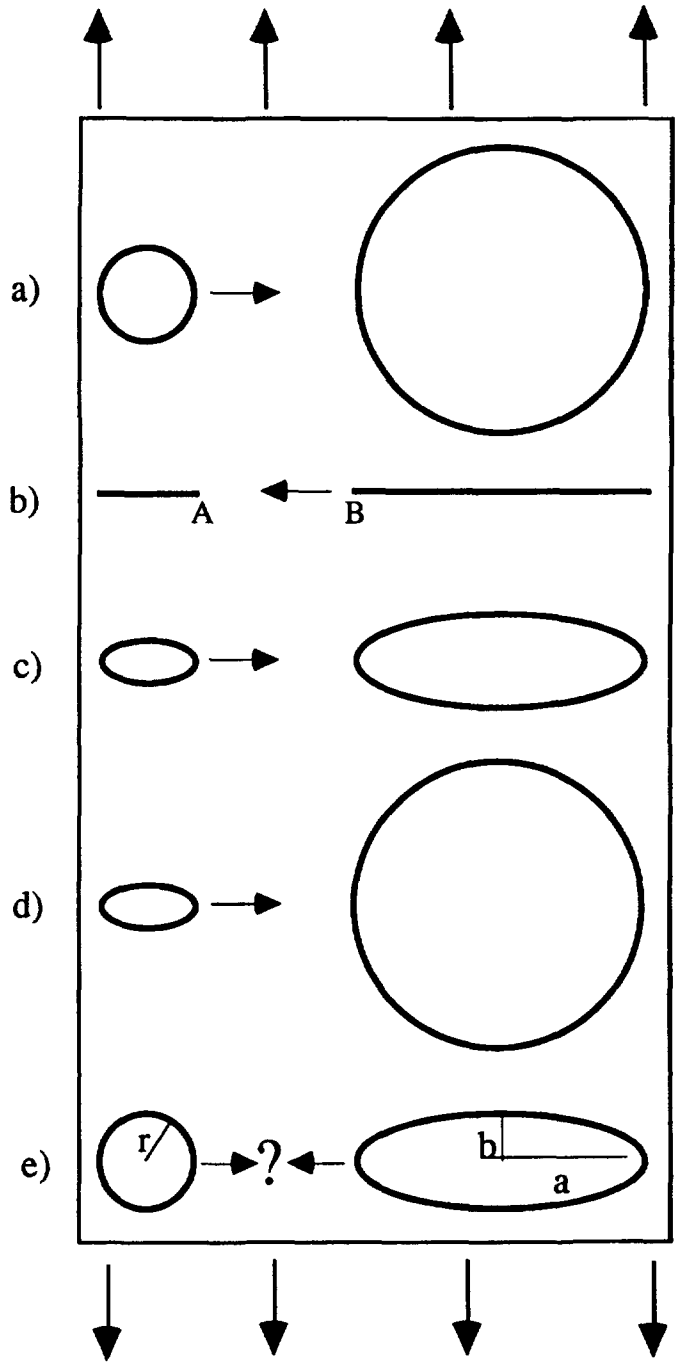


Fig. 11. Stress concentrations for interacting holes of diverse eccentricities. Arrows indicate the directions of likely fracturing (from the defect where the concentration is the highest, towards the "attracting" neighbor): (a) circular holes; (b) cracks; (c) elliptical holes of identical eccentricity but different sizes; (d) small elliptical hole and large circular hole; (e) large elliptical hole and small circular hole.

the larger crack. This result is explained by the fact that, for an isolated crack of length $2l$ under remote tension $p$, $K_I = p\sqrt{\pi l}$ is higher for a larger crack; this factor is dominant, as compared to the amplifying impact of interaction.

These two limiting cases indicate that, for interacting *elliptical* holes, the pattern is not obvious and will depend on eccentricities of the holes and on spacings between them.

In the case of collinear holes of unequal sizes of the same eccentricity $\lambda = b/a \leqslant 1$ under remote tension, the highest hoop stress will occur at the smaller hole boundary (Fig. 11c). Indeed, the stress concentration factor for a single isolated hole $1+2/\lambda$ is the same for both holes. Since the amplifying impact of a larger hole on the smaller one is stronger than vice versa, the highest hoop stress occurs at the smaller hole boundary. A similar conclusion, obviously, holds for the system "larger hole with larger $\lambda$–smaller hole with smaller $\lambda$" (Fig. 11d).

A less obvious case is the configuration "larger hole with smaller $\lambda$–smaller hole with larger $\lambda$" (Fig. 11e). The point of the highest hoop stress is determined by the competition of two effects: (1) in the absence of interaction, the hole with smaller eccentricity experiences a higher stress concentration and (2) the larger hole produces a stronger impact on the smaller one than vice versa. Figure 12a shows the eccentricity $\lambda$ of a larger hole interacting with a small circular hole for which the situation is "neutral": the stress concentrations are the same at both holes. (The major axis $a$ of the larger hole remains equal to 3 diameters of the smaller hole while its minor axis $b$ is varied.) Points below (above) the curve correspond to the highest hoop stress occurring at the boundary of the larger (smaller) hole. At larger spacings between the holes, the interaction weakens and even a slight ellipticity of the larger hole ($\lambda$ close to 1) results in shifting of the point of the highest stress from the smaller hole to the larger one.

Figure 12b further illustrates this phenomenon. It shows three configurations (drawn in scale) that are "neutral" (the maximal hoop stress is the same on both holes, and equal to 3.236, 4.315, 8.224 of $p$, correspondingly). Reduction (increase) of the spacing between holes, as compared to the "neutral" configuration, would result in shifting of the point of maximal hoop stress to the smaller (larger) hole.

## 6. INTERACTION OF A LARGE HOLE WITH AN ARRAY OF SMALL HOLES

Consider now the interaction of a large hole with an array of smaller ones. This configuration may be relevant for porous media. As shown by Tsukrov and Kachanov (1994), the interaction between small holes can be ignored in the first approximation, as compared to the "large hole–small hole" interactions. Then the results for two interacting holes can be utilized. Assuming that fracturing starts at the point of the highest tensile hoop stress, Fig. 13 shows the likely microfracturing patterns.

For a crack interacting with micropores, fracture will initiate at the crack tip (Fig. 13a).

If the shape of the larger hole is close to a circle, then micropores (and microcracks) will advance towards the larger hole, independently of their shapes (Fig. 13b).

For a strongly elongated hole (small $\lambda$) interacting with more or less circular microholes, the pattern of fracture initiation will depend on the spacing between the holes. If the distances between the large hole and the microholes are small, then the smaller holes will fracture first and, presumably, will crack towards larger hole (Fig. 13c). At larger spacings when the interaction effect is weak, fracture will initiate at the larger hole (Fig. 13d).

Figure 14a,b show a large elliptical hole (of eccentricity 1/3) interacting with two sample sequences of microhole arrays of diverse eccentricities; in each sequence new microholes are added in steps, as shown. Points of the highest hoop stress on holes are marked. A number of physically interesting observations can be made:

1. The results shed some light on the problem of *short range* vs *long range* interactions. In the problem of macrocrack–microcrack array interactions, the short range interactions are dominant, in the sense that the impact of microcracks on SIF at the main crack tip is dominated by the influence of several closest neighbors (Kachanov *et al.*, 1990). This dominance of the short range interactions becomes less pronounced in the case of microholes, as seen from Figs 14a,b: a limited number of far-away neighbors changes noticeably the stress concentration at the boundary of the large hole, although the closest microholes still produce the dominant effect.

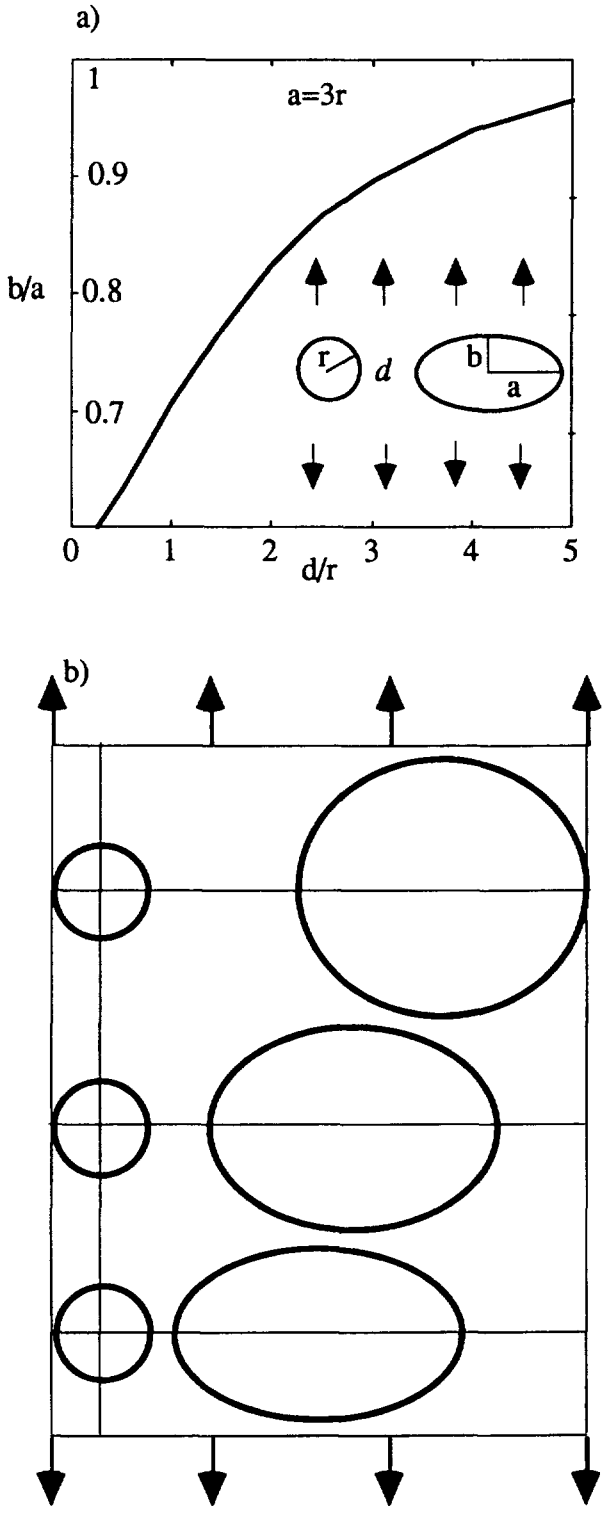


Fig. 12. Examples of "neutral" configurations for various combinations of eccentricities and spacings (maximal stress concentrations at the interacting holes are equal).

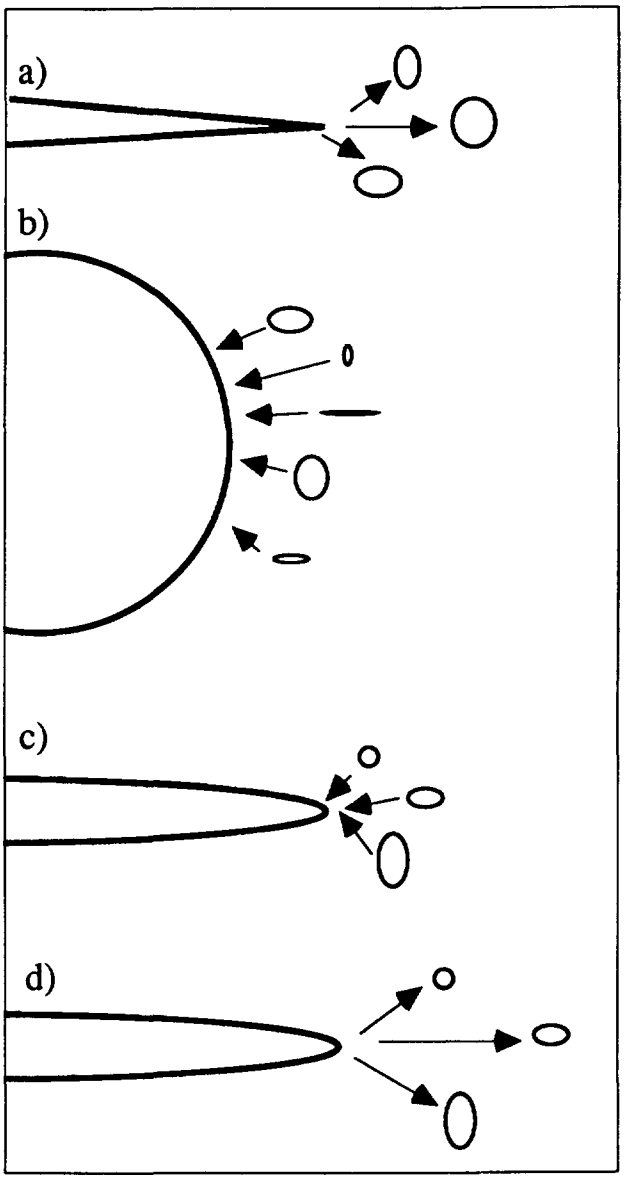


Fig. 13. Likely microfracturing patterns for (a) crack and microholes; (b) large circular hole and microholes of various shapes; (c) strongly elongated hole and microholes at large distances; (d) strongly elongated hole and microholes at small distances. Arrows show the directions of likely fracture propagation.

2. In contrast with the case of cracks (where it is usually the larger crack that has the highest SIF in the stress amplifying configuration) it is the small holes where the highest hoop stress is likely to occur. This is related to the fact that the impact of the larger hole on a smaller one is higher than vice-versa (see discussion in Section 5). This seems to have interesting physical implications: the presence of a large hole will enhance microfracturing of small holes.

3. It is not necessarily the most elongated microhole where the highest hoop stress occurs. As seen from Fig. 14a, the highest hoop stress occurs on the microhole with the eccentricity 2/3, in spite of the presence of much more elongated microholes (of eccentricity 1/3). This is due to the fact that the mentioned microhole experiences the strongest amplifying influence of the main hole.

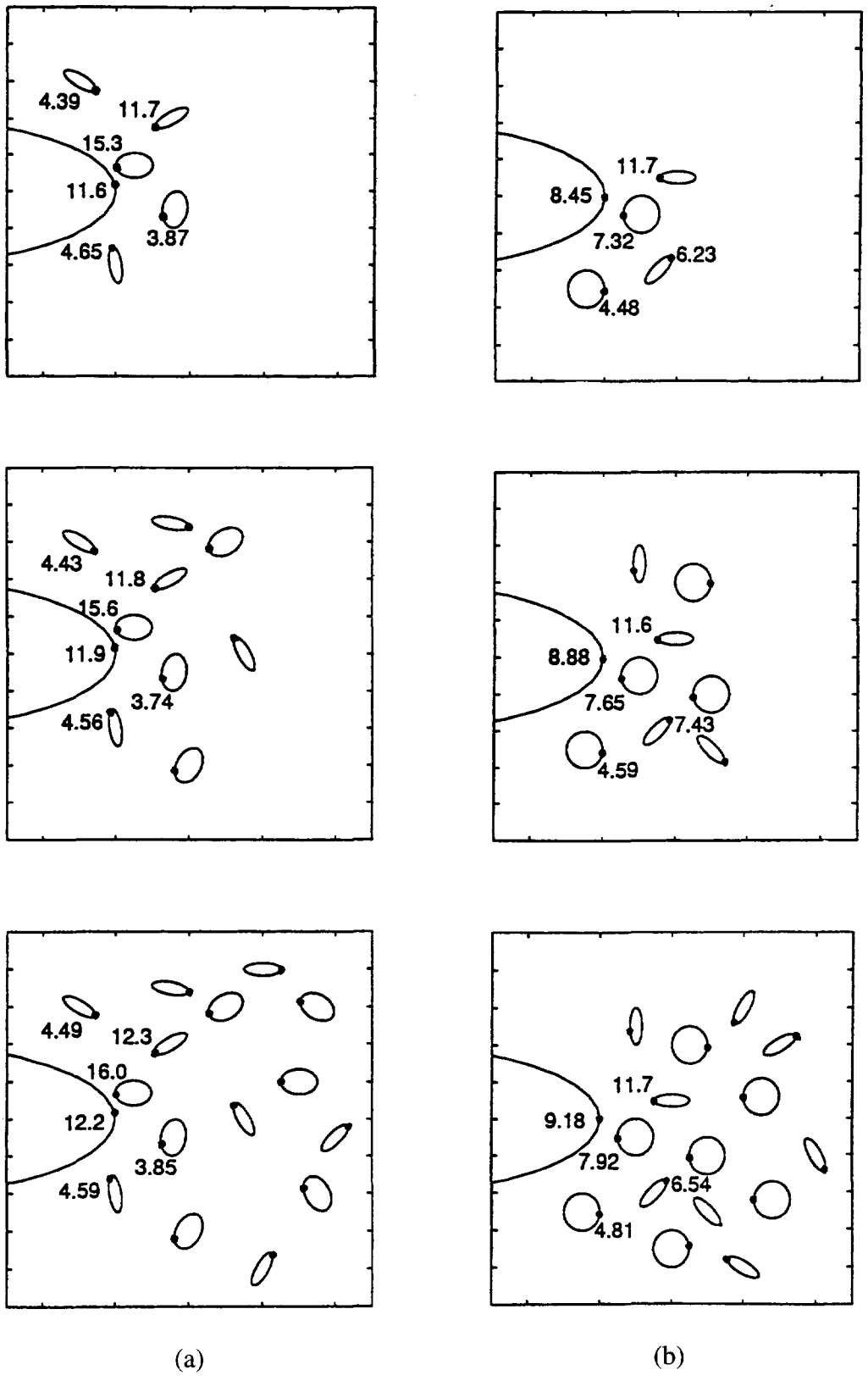


Fig. 14. Large elliptical hole (of eccentricity 1/3) interacting with sample arrays of small holes of diverse eccentricities. The remote tension is normal to the major axis of the large hole. The points of maximal hoop stress (where the fracturing is likely to start) and the values of stress concentration factors at them are shown.

## 7. EXTREMAL PROPERTIES OF SLIGHTLY ASYMMETRIC CONFIGURATIONS

An interesting (and counterintuitive) result of our analysis is that the interaction effects may be maximal not in the ideally symmetric arrangements but in the configurations where the symmetry is slightly perturbed. A similar phenomenon for cracks was analyzed by Kachanov (1993).

The underlying physical mechanism is best explained in the example of cracks, for which the phenomenon is most strongly pronounced. Consider two collinear cracks of equal length under remotely applied uniform tension normal to the cracks. If the right crack is rotated about its center on an angle $\phi$, the SIF $K_I$ at "inner" tip of the left crack is maximal not at $\phi = 0$ (as may be intuitively expected) but at $\phi \approx 15^\circ$. The explanation is that this SIF is affected by both modes *I* and *II* on the right crack. The impact of the mode *I* (mode $I \to I$ interaction) is, obviously, maximal at $\phi = 0$, but this means that its rate of change with respect to $\phi$ is zero at $\phi = 0$, so that its reduction due to a moderately small rotation $\phi$ is small. On the other hand, the impact of mode *II* on the right crack (non-existent at $\phi = 0$), i.e., mode $II \to I$ interaction, increases at finite rate as $\phi$ increases. Therefore, the *combined* impact of both modes is maximal at non-zero $\phi$.

Thus, the phenomenon is due to "mixed mode" interactions that appear due to perturbations of symmetry. It is clear, therefore, that the phenomenon is general (applies to configurations other than the collinear one): *perturbations of symmetry that give rise to mixed mode interactions intensify interactions* (provided the perturbation remains moderately small). In the case of collinear cracks, for example, perturbations other than rotations (parallel shift, etc.) lead to a similar intensification of interactions. One can easily construct a number of similar configurations (for example, a rectangular periodic array of cracks where either orientations or positions of defects are slightly perturbed). The excess of stress concentrations in configurations with perturbed symmetry over their values in the ideally symmetric configurations may be quite noticeable.

For holes, the phenomenon is similar, but it is not as strongly pronounced. Consider, for example, two collinear elliptical holes and let the symmetry be perturbed by rotating the right hole (Fig. 15a). The stress concentration on the left hole is maximal not at $\phi = 0$, but at $\phi \approx 7^\circ$ (for holes of eccentricity $b/a = 1/3$).

A similar phenomenon holds in 3-D configurations. It has many more manifestations due to a larger variety of possible geometrical asymmetries; see Kachanov (1993) for details.

These observations on extremal properties of slightly asymmetric configurations may have some physical implications, particularly for crack-like slits (although such considerations should be viewed as speculative at this point). If one assumes that the system tends to maximize the energy release rate (a combination of SIFs, $K_I$ and $K_{II}$), then the initially symmetric configurations will tend to deviate from symmetry in the course of crack propagation, in order to "pick up" the mixed mode interactions that increase SIFs. For example, in the configuration of two collinear cracks under remote tension, the cracks do not grow towards each other along the straight line but deviate from it, "avoiding each other". A rather complex mathematical discussion of this problem was given by Melin (1983). A simpler explanation may, possibly, be suggested: the deviation from symmetry leads to mixed mode interactions that maximize the energy release rate.

Asymmetry of some naturally occurring crack patterns may, possibly, be related to the same tendency of the system to maximize the energy release rate by deviating from symmetry and thus picking up contributions from mixed mode interactions.

In the case of *holes*, the phenomenon may have yet another manifestation: the point of maximal stress concentration may shift in an unexpected direction as the symmetry is perturbed. As an example, consider a large elliptical hole interacting with a small circular hole; the smaller hole is shifted upwards from the collinear arrangement (Fig. 15b). The discussed phenomenon manifests itself in two ways: (1) the maximal hoop stress on the smaller hole occurs when the smaller hole is slightly shifted upwards (in spite of the fact that this increases the spacing between the holes) and (2) the point of the maximal hoop stress on the smaller hole is located above the point B (contrary to intuition).

*Acknowledgment*—This research was supported by the Army Research Office through a grant to Tufts University. The second author (Mark Kachanov) acknowledges the von Humboldt research award for senior U.S. scientists.

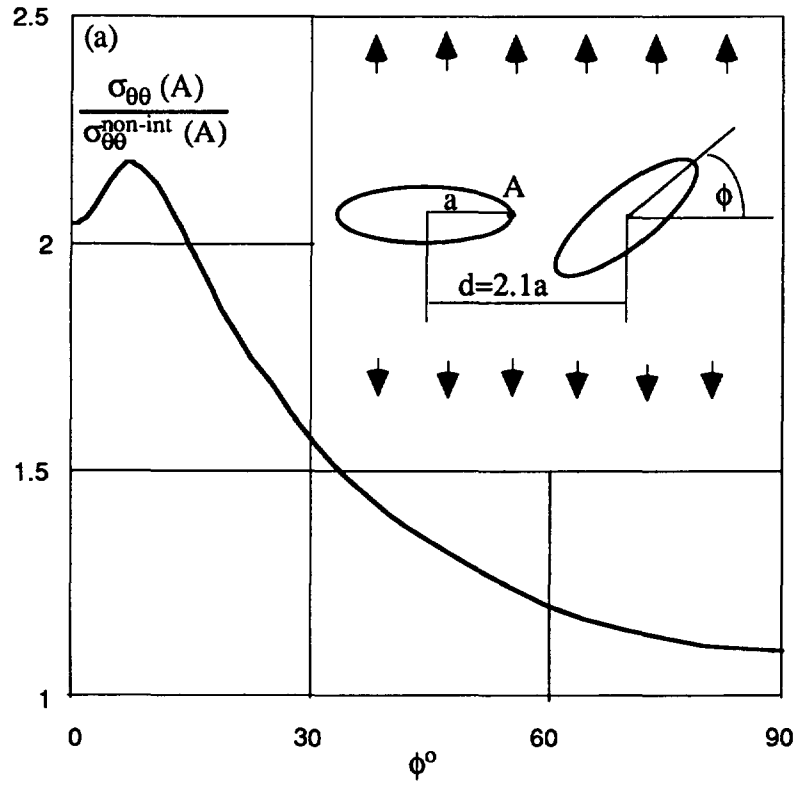


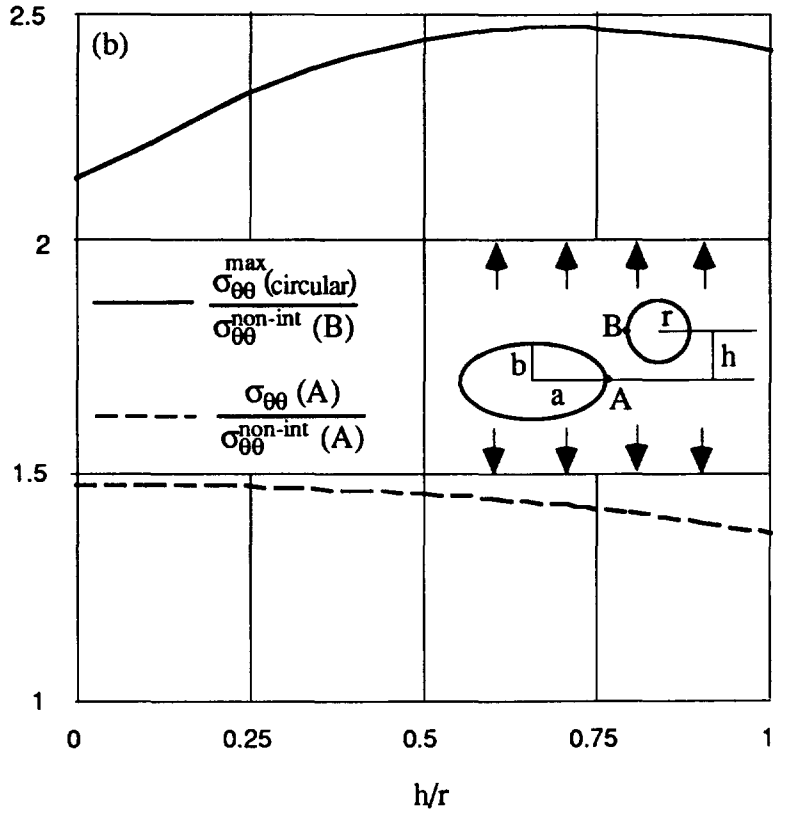


Fig. 15. Extremal properties of slightly asymmetric configurations: (a) perturbed collinear configuration of identical elliptic holes: maximal stress concentration occurs not in the symmetric configuration $\phi = 0$ (as may be intuitively expected), but in the configuration of perturbed symmetry ($\phi \approx 7°$, for the eccentricity $b/a = 1/3$); (b) perturbed collinear configuration of an elliptical hole and a small circular hole ($a = 6r$, $b = 2r$, horizontal distance between $A$ and $B = = 0.5r$): maximal stress concentration at the circular hole occurs not when $h = 0$ but at $h/r \approx 0.7$. Stresses are normalized to their values for non-interacting (isolated) holes.

## REFERENCES


Duan, Z. P., Kienzler, R. and Herrmann, G. (1986). An integral equation method and its application to defect mechanics. *Journal of Mechanics and Physics of Solids* **34,** 539–561.

Dundurs, J. and Hetenyi, M. (1961). The elastic plane with a circular insert, loaded by a radial force. *Journal of Applied Mechanics* **28,** 103–111.

Edwards, R. H. (1951). Stress concentrations around spheroidal inclusions and cavities. *Journal of Applied Mechanics* 19–31.

Fond, C., Flejou, J.-L. and Berthaud, Y. (1995). Interaction between cracks and circular holes in two-dimensional linear elastic media. *European Journal of Mechanics A/Solids* **14,** 73–96.

Green, A. E. and Zerna, W. (1954). *Theoretical Elasticity*, Oxford University Press.

Haddon, R. A. W. (1967). Stresses in an infinite plate with two unequal circular holes. *Quarterly Journal of Mechanics and Applied Mathematics* **20,** 277–291.

Hetenyi, M. and Dundurs, J. (1962). The elastic plane with a circular insert, loaded by a tangentially directed force. *Journal of Applied Mechanics* **28,** 362–368.

Horii, H. and Nemat-Nasser, S. (1985). Elastic fields of interacting inhomogeneities. *International Journal of Solids and Structures* **21,** 731–745.

Hu, K. X., Chandra, A. and Huang, Y. (1993). Multiple void-crack interaction. *International Journal of Solids and Structures* **30,** 1473–1489.

Hwu, C. and Liao, C. Y. (1994). A special boundary element for the problems of multi-holes, cracks and inclusions. *Computers and Structures* **51,** 23–31.

Inglis, C. E. (1913). Stresses in a plate due to the presence of cracks and sharp corners. *Transactions of the Institute of Naval Architects* 219–230.

Kachanov, M. (1993). Elastic solids with many cracks and related problems. In *Advances in Applied Mechanics* Vol. 3, (eds Hutchinson, J. W. and Wu, T. Y.), Academic Press, pp. 259–445.

Kachanov, M., Montagut, E. and Laures, J. P. (1990). Mechanics of crack-microcrack interactions. *Mechanics of Materials* **10,** 1059–1071.

Kolosov, G. V. (1909). *On an Application of Complex Function Theory to a Plane Problem of the Mathematical Theory of Elasticity*, Yuriev Publ. Co.

Ling, C. B. (1947). On the stresses in a plate containing two circular holes. *Journal of Applied Physics* **19,** 77–82.

Maugis, D. (1992). Stresses and displacements around cracks and elliptical cavities: exact solutions. *Journal of Engineering Fracture Mechanics* **43,** 217–255.

Melin, S. (1983). Why do cracks avoid each other? *International Journal of Fracture* **37,** R55–R60.

Muskhelishvili, N. I. (1919). Sur l'integration de l'equation biharmonique. *Izvestia Rossiyskoi Academii Nauk* 663–686 (in French).

Muskhelishvili, N. I. (1953). *Some Basic Problems of the Mathematical Theory of Elasticity*, Noordhoff, Groningen-Holland.

Rajiyah, H. and Atluri, S. N. (1989). Evaluation of K-factors and weight functions for 2-D mixed mode multiple cracks by the boundary element alternating method. *Engineering Fracture Mechanics* **32,** 911–922.

Rubinstein, A. A. (1986). Macrocrack-microdefect interaction. *Journal of Applied Mechanics* **53,** 505–510.

Savin, G. N. (1961). *Stress Concentrations Around Holes*, Pergamon Press, London.

Sokolnikoff, I. S. (1956). *Mathematical Theory of Elasticity*, McGraw-Hill.

Tsukrov, I. and Kachanov, M. (1994). Stress concentrations and microfracturing patterns for interacting elliptical holes. *International Journal of Fracture* **68,** R89–R92.

Yokobori, T., Ohashi, M. and Ichikawa, M. (1965). The interaction of two collinear assymetrical elastic cracks. *Reports of the Research Institute for Strength and Fracture of Materials*, **1,** 33–39.

Zimmerman, R. W. (1988). Stress singularity around two nearby holes. *Mechanics Research Communications* **15,** 87–90.

Zimmerman, R. W. (1991). *Compressibility of Sandstones*, Elsevier, Amsterdam.